Insulated Nonradiative Dielectric Waveguide for Millimeter-Wave Integrated Circuits

TSUKASA YONEYAMA, MEMBER, IEEE, SADAO FUJITA, AND SHIGEO NISHIDA, SENIOR MEMBER, IEEE

Abstract—**An improved version of the nonradiative dielectric waveguide (NRD-guide), called an insulated nonradiative dielectric waveguide, is proposed for millimeter-wave integrated circuits. This dielectric waveguide can overcome some difficulties which arise when high dielectric material is used in the NRD-guide. Guide wavelengths and transmission losses were measured at 50 GHz and compared with theory. In addition, some basic circuit components such as bends, ring resonators, chip resonators, and T-junctions were fabricated on the basis of the insulated NRD-guide and tested to confirm their usefulness in millimeter-wave integrated circuits. The fabricated components operated as expected without suffering from any appreciable radiation at curved sections and discontinuities.**

I. INTRODUCTION

THE NONRADIATIVE dielectric waveguide (NRD-guide) has been proposed for use in millimeter-wave integrated circuits [1] and studied using polystyrene dielectric exclusively [2], [3]. Though high-dielectric materials such as Stycast (trade name, $\epsilon_r = 10.5$) and alumina ($\epsilon_r = 8.5$) are preferable in view of the small circuit size, their use in NRD-guide fabrication entails some difficulties. First of all, the dielectric strips must be unusually wide in one dimension of the cross section and thin in the other. The transverse dimensions of a typical Stycast strip are 2.7 mm $\times$ 0.86 mm at 50 GHz. Such a flat strip wastes more dielectric material than necessary and is difficult to fabricate with reasonable accuracy. Another disadvantage of using high-dielectric strips in the NRD-guide is the narrow frequency band for single-mode operation which is limited by the presence of the extra E_{12}^x mode (named according to the image guide convention). In order to overcome these difficulties and to simultaneously attain some reduction in transmission loss, an insulated nonradiative dielectric waveguide is proposed in this paper.

In the insulated NRD-guide, high-dielectric strips are sandwiched between low-dielectric overlays on conducting plates. These overlays are different from that of the insulated image guide in that they not only reduce transmission losses, but also suppress generation of unwanted higher modes. Key requirements for the insulated NRD-guide to prevent radiation from being generated at bends and discontinuities are that the separation of the conducting plates be smaller than a certain critical value determined by the dielectric constant and thickness of the overlays (see (6)) and that the electric field of the operating mode be parallel to the conducting plates. This improved design of dielectric waveguide can successfully eliminate most difficulties associated with the high-dielectric NRD-guide without spoiling the nonradiative nature of the waveguide at all, as will be explained later.

Insulated NRD-guides were fabricated using Stycast and alumina to measure guide wavelengths and transmission losses at 50 GHz. Since the materials were selected only from a standpoint of high-dielectric constant and ease of fabrication, their loss tangents were not necessarily very small, and hence the transmission losses were unexpectedly large. But, the theory predicts that it is not difficult to reduce the transmission loss of the insulated NRD-guide below 2.5 dB/m, if high-quality alumina (loss tangent $\simeq 10^{-4}$) is used.

Some basic circuit components such as bends, ring resonators, chip resonators, and T-junctions were fabricated to test the applicability of the insulated NRD-guide to millimeter-wave integrated circuits. The fabricated components worked in a predictable manner, since undesirable radiation was suppressed below a tolerable level. Thus, the insulated NRD-guide was confirmed to be a very convenient structure for constructing miniaturized millimeter-wave integrated circuits with high-dielectric material such as Stycast and alumina.

II. OPERATION DIAGRAM

Fig. 1 shows a structural view of the insulated NRD-guide. The top and bottom plate separation is a, the transverse dimensions of the dielectric strip are $b \times c$, and dielectric constants of the strip and the overlays are ϵ_{r2} and ϵ_{r1}, respectively. The dielectric constant ϵ_{r1} can be unity in the special case where the low-dielectric overlays are replaced with air layers.

In order to analyze the insulated NRD-guide, the effective dielectric constant (EDC) method will be used. In the presence of the conductive boundaries, however, different sequences of applying the EDC method often cause a substantial difference in the final results [4]. In this paper, the EDC method is applied in the order depicted in Fig. 2. The slab waveguide of thickness b is solved first for TM modes to obtain the effective dielectric constant

$$\epsilon_{re} = \epsilon_{r2} - \frac{q^2}{k_0^2} \tag{1}$$

Manuscript received March 30, 1983; revised August 4, 1983.

T. Yoneyama and S. Nishida are with the Research Institute of Electrical Communication, Tohoku University, Katahira 2-1-1, Sendai, 980 Japan.

S. Fujita is with the Opto-Electronics Research Laboratory, NEC Cooperation, Japan.

0018-9480/83/1200-1002$01.00 ©1983 IEEE

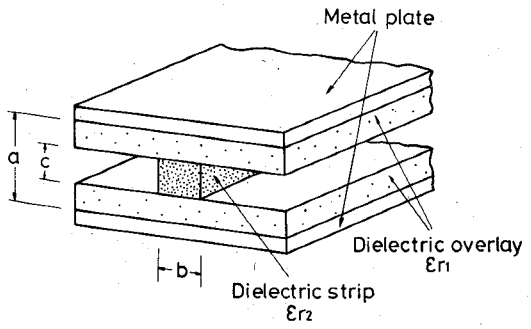

Fig. 1. Structural view of insulated nonradiative dielectric waveguide.

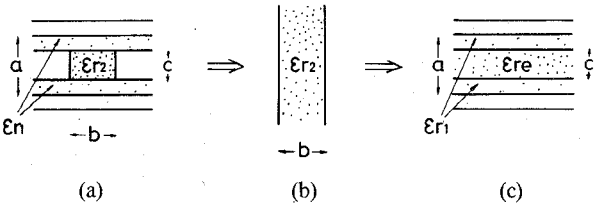

Fig. 2. Decomposition of insulated nonradiative dielectric waveguide into its equivalent two-dimensional waveguides for applying the effective dielectric constant (EDC) method.

where k_0 is the free-space wavenumber and q is the solution to the characteristic equations

$$q\tan\left(\frac{qb}{2}\right)=\epsilon_{r2}\sqrt{(\epsilon_{r2}-1)k_0^2-q^2}\,, \qquad \text{for even modes} \tag{2a}$$

$$-q\cot\left(\frac{qb}{2}\right)=\epsilon_{r2}\sqrt{(\epsilon_{r2}-1)k_0^2-q^2}\,, \qquad \text{for odd modes.} \tag{2b}$$

Then, a hypothetical three-layered slab sandwiched between the conducting plates as shown in Fig. 2(c) is solved for TE modes to derive the characteristic equations

$$u\tan\left(\frac{uc}{2}\right)=w\coth\left(w\frac{a-c}{2}\right), \qquad \text{for even modes} \tag{3a}$$

$$-u\cot\left(\frac{uc}{2}\right)=w\coth\left(w\frac{a-c}{2}\right), \qquad \text{for odd modes} \tag{3b}$$

where

$$u^2+w^2=(\epsilon_{re}-\epsilon_{r1})k_0^2. \tag{3c}$$

Once the above equations are solved, the propagation constant of the original waveguide in Fig. 2(a) can be calculated by

$$\beta=\sqrt{\epsilon_{re}k_0^2-u^2}\,. \tag{4}$$

Therefore, the cutoff condition for any specific mode is given by

$$\beta=0 \text{ or } u=\sqrt{\epsilon_{re}}\,k_0. \tag{5}$$

The reversed sequence is traced in the analysis of the trapped image guide [4]. The present approach may also be justified by the fact that it yields the exact solution when the low-dielectric overlays tend to zero in thickness

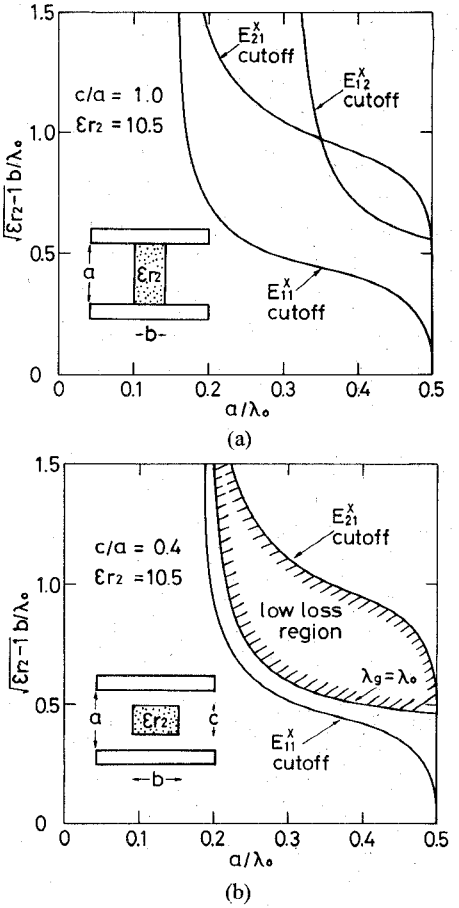

Fig. 3. Operation diagrams of (a) nonradiative and (b) insulated nonradiative dielectric waveguides. Stycast ($\epsilon_{r2}=10.5$) is assumed for dielectric strip material and air layers ($\epsilon_{r1}=1.0$) for overlays.

(NRD-guide). Another important requirement for the insulated NRD-guide is its radiation suppression capability. By imposing the cutoff condition for TE waves between the conducting plates covered with overlay, the condition for radiation suppression is obtained as

$$\tan\left(\pi\frac{c}{\lambda_0}\right)=\sqrt{\epsilon_{r1}}\,\cot\left(\sqrt{\epsilon_{r1}}\,\pi\frac{a-c}{\lambda_0}\right). \tag{6}$$

Equations (5) and (6) are fundamental for designing the insulated NRD-guide.

Operation diagrams for the NRD-guide ($c/a=1.0$) and the insulated NRD-guide ($c/a=0.4$) are presented in Fig. 3(a) and (b), respectively. The operation diagram represents critical curves for both the guided modes and radiated waves as given by (5) and (6). In both the figures, Stycast ($\epsilon_{r2}=10.5$) is assumed for strip material and air layers for the overlays ($\epsilon_{r1}=1.0$). Then, the critical curve for radiated waves is a vertical line at $a/\lambda_0=0.5$. It was decided to name modes of the insulated NRD-guide according to the image guide convention with the x-axis parallel to the conducting plates.

According to the meaning of the operation diagram, a mode is propagating above its critical curve and cutoff below it. Thus, the E_{11}^x mode is the only propagating mode in the region bounded by all critical curves shown in Fig. 3(a) and (b). As shown in Fig. 3(a), a considerable area is

cut away by the critical curve of the E_{12}^x mode. This results in a substantial reduction of the frequency band for single-mode operation. In the insulated NRD-guide, however, such a reduction of the frequency band never arises, as can be seen in Fig. 3(b). The reason for this is that the critical curve for the unwanted E_{12}^x mode is shifted up. This occurs because the effective dielectric constant for the E_{12}^x mode is substantially reduced in the insulated NRD-guide since two field maxima associated with this mode are away from the high-dielectric region toward the low-dielectric overlays. On the contrary, the E_{11}^x and E_{21}^x modes are hardly affected by the presence of the overlays since the field maximum of each mode is at the center of the high-dielectric core. Thus, one of the disadvantages of the high-dielectric NRD-guide is removed and the bandwidth is substantially improved.

Typical dimensions of the Stycast NRD-guide can be determined from the operation diagram as $a = c = 2.7$ mm and $b = 0.86$ mm at 50 GHz, while those of the insulated NRD-guide are determined as $a = 2.7$ mm, $b = 1.45$ mm, and $c = 1.08$ mm. It can be seen that the dielectric strip in the insulated NRD-guide is more compact in cross section and hence less wasteful of dielectric material and easier to fabricate than that in the NRD-guide. This overcomes another disadvantage of the high-dielectric NRD-guide.

If the guide wavelength of the E_{11}^x mode is smaller than the wavelength of a plane wave in the low-dielectric medium, the fields decay toward the conducting plates in an exponential manner so that a reduction of the conduction loss can be expected. This condition is fulfilled in the hatched low-loss region in Fig. 3(b). At this point of discussion, it is important to note that for the insulated NRD-guide with Teflon overlays ($\epsilon_{r1} = 2.04$), the conducting plate separation must be smaller than $0.43\lambda_0$ to suppress radiation when $c/a = 0.4$. Although Teflon overlays are convenient to firmly hold dielectric strips in the waveguide, this reduced plate separation causes an increase of the transmission loss.

III. Measurements

By using Stycast and alumina as high-dielectric material, insulated NRD-guides were fabricated to measure guide wavelengths and transmission losses at 50 GHz. Preliminary measurements on NRD-guide and rod guide structures for which accurate characteristic equations and loss equations are known have shown that the material constants of Stycast and alumina are $\epsilon_{r2} = 10.5$, $\tan\delta = 3.8 \times 10^{-3}$ and $\epsilon_{r2} = 8.5$, $\tan\delta = 10^{-3}$, respectively. Considering these values, the materials are not necessarily satisfactory for millimeter-wave applications, but they may still be used for examining basic properties of the insulated NRD-guide.

A. Transition

A transition between a metal waveguide and an insulated NRD-guide was constructed in the configuration shown in Fig. 4. To facilitate fabrication, no tapers were provided at the ends of the strip. For support within metal waveguides, the dielectric strip was anchored in a hole drilled in a Teflon piece, with the same transverse dimensions as the standard metal waveguide. This piece was 3.1 mm in length, and was backed by a similar Teflon piece 1.1 mm in length. Since these Teflon pieces serve as impedance transformers, their lengths had to be carefully adjusted. The waveguide was provided with two rectangular metal fins, 5 mm in length and 2.7 mm in height, which were centered on the edges of the broad walls, flared out by about 30°, and inserted between the conducting plates to precisely maintain the plate separation. Though the structure is simple, this transition worked very well, and the return loss was measured as being better than 14 dB, at least over the 2-GHz frequency band of a mechanically tuned klystron oscillator.

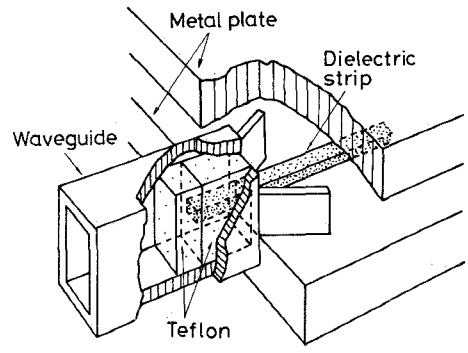

Fig. 4. Structure of transition used in measurements.

B. Guide Wavelength

In the measurement of guide wavelength, the insulated NRD-guide was terminated by a metal waveguide short by way of the transition to create clear standing wave patterns along the dielectric strip. The electric field was probed by an electrically small unipole antenna consisting of the inner conductor of a semi-rigid cable 0.8 mm in diameter. The outer surface of the cable was coated with a very thin lossy material to suppress undesirable interference. The dimensions of the tested guides were $a = 2.7$ mm, $b = 1.45$ mm, and $c = 1.08$ mm for Stycast and $a = 2.7$ mm, $b = 1.5$ mm, and $c = 1.0$ mm for alumina. The guide wavelength is shown in Fig. 5 as a function of frequency. Solid curves represent theoretical values calculated by the EDC method. Agreement between theory and measurements is excellent within practical accuracy. The measurements revealed that the guide wavelength and dispersion of the insulated NRD-guide are not much different from those of the rod guide so long as modes in both the waveguides are well above cutoff. This is quite in contrast to the NRD-guide and implies that the metal plates, though suppressing radiation, hardly affect the guided mode of the insulated NRD-guide.

C. Transmission Loss

Transmission losses were measured by comparing transmission coefficients of two insulated NRD-guides of different lengths, 40 mm and 70 mm. Measured data of the transmission coefficients for insulated NRD-guides are

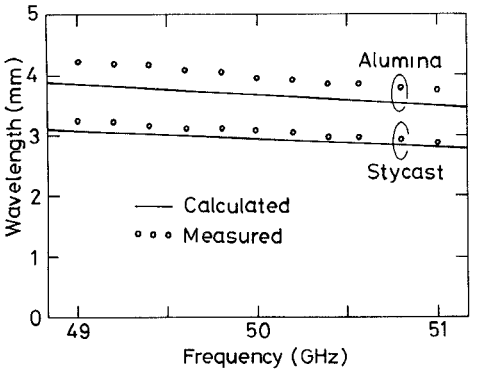

Fig. 5. Calculated and measured guide wavelength of insulated nonradiative dielectric waveguide. Stycast ($\epsilon_{r2}=10.5$) and alumina ($\epsilon_{r2}=8.5$) were used for dielectric strips.

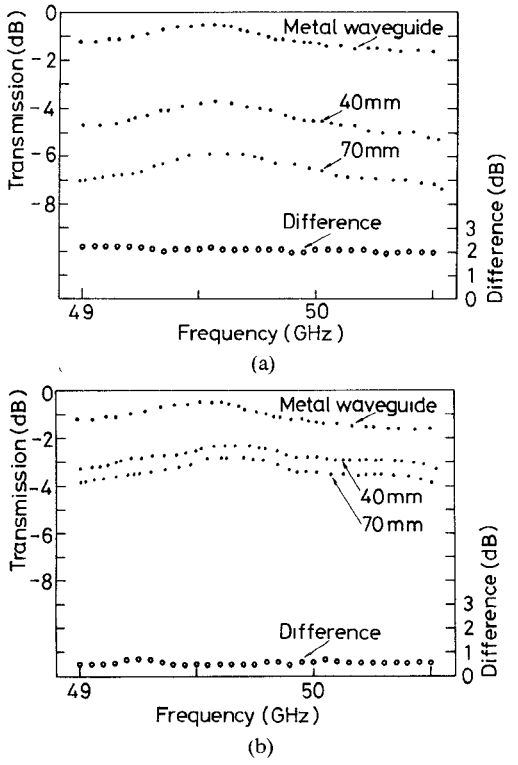

Fig. 6. Measured transmission coefficients of (a) Stycast and (b) alumina insulated nonradiative dielectric waveguides. The transmission coefficient of a standard metal waveguide 40 mm in length is also shown for comparison.

shown in Fig. 6(a) and (b) together with those for the metal waveguide, which was 40 mm in length. Difference between the transmission coefficients of 70 mm and 40 mm long guides gives a transmission loss over a guide length of 30 mm. The measured transmission loss for the Stycast guide was 69 dB/m. The corresponding theoretical value, which is calculated by means of the EDC method, is 69.9 dB/m, assuming the conducting plates to be brass ($\sigma=1.7\times10^{7}$ S/m). This value consists of 69.4 dB/m dielectric loss and 0.5 dB/m conduction loss. Therefore, if less lossy dielectric material is used, a reduction of the transmission loss will be attained. In fact, this can be understood by examining data for the alumina guide in Fig. 6(b). The measured transmission loss was estimated to

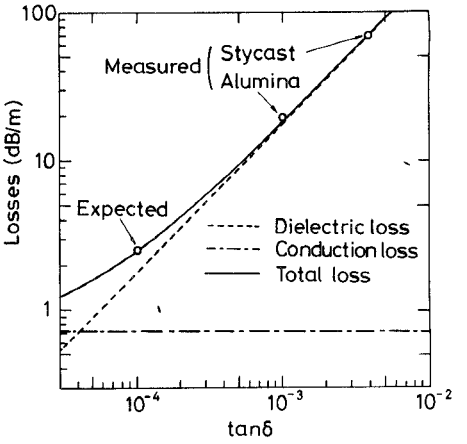

Fig. 7. Theoretical transmission loss of insulated nonradiative dielectric waveguide at 50 GHz as a function of the loss tangent of a dielectric material ($\epsilon_{r2}=9.5$). Measured values for Stycast ($\tan\delta=3.8\times10^{-3}$) and alumina ($\tan\delta=10^{-3}$), and an expected value for high-quality alumina ($\tan\delta=10^{-4}$) are also shown.

be 19 dB/m in this case. The theoretical value is 17.2 dB/m, which includes a 16.3 dB/m dielectric loss and a 0.9 dB/m conduction loss. Since the dielectric loss is proportional to the loss tangent of the material, the transmission loss can be expected to be further reduced, if high-quality alumina is used.

This prediction can be verified by examining Fig. 7, in which transmission loss of an insulated NRD-guide is plotted against the loss tangent of the dielectric strip at 50 GHz. Measured values of transmission loss of Stycast and alumina insulated NRD-guides are also included for the purpose of comparison. Though dielectric constants of Stycast and alumina are slightly different from that assumed in calculation ($\epsilon_{r2}=9.5$; the average of those of Stycast and alumina), theory agrees with measurements. Tracing the total loss curve toward the small loss tangent, a 2.5 dB/m transmission loss is reached at $\tan\delta=10^{-4}$, such low-loss alumina being currently available.

D. Bends

An outstanding feature of the insulated NRD-guide is its capability to suppress radiation at sharp bends. In order to confirm this, bending losses of two Stycast 90° bends, one with a curvature radius of 6 mm and the other with a curvature radius of 2 mm, were measured. The larger curvature radius is about twice as large as the guide wavelength, while the smaller one is two-thirds of the guide wavelength. The curved strips were supported at the transitions and suspended between the conducting plates. Measurements of bending losses were carried out by comparing transmission coefficients of bends with those of straight strips of the same length. Bending losses of open dielectric waveguide bends with one or both of the conducting plates removed, were also measured for purposes of comparison.

Measured bending losses are shown in Fig. 8(a) and (b) as a function of frequency for the bends with curvature radii of 6 mm and 2 mm, respectively. Since the dielectric strips were small in size, their setting was very critical. Considering this handicap, observed bending losses of the

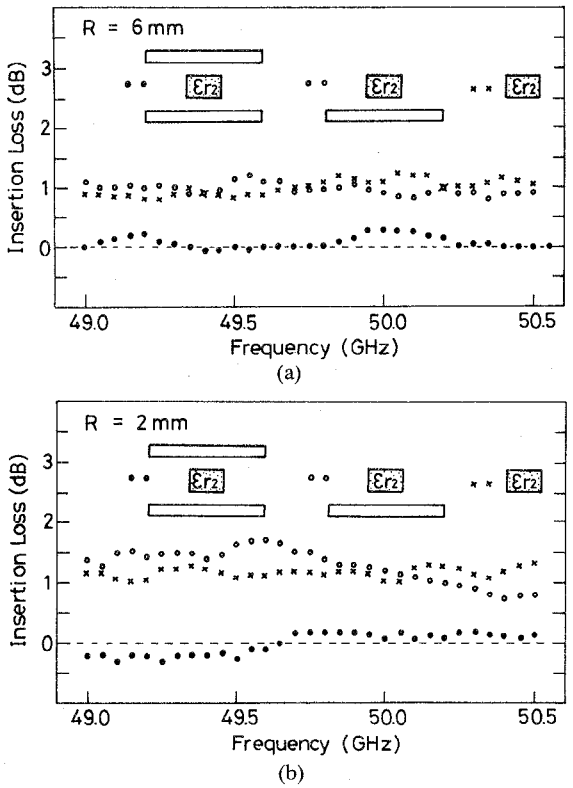

Fig. 8. Measured insertion losses of insulated nonradiative dielectric waveguide 90° bends having curvature radii of (a) 6 mm and (b) 2 mm, respectively. Insertion losses for other types of open dielectric waveguide bends are also included for comparison.

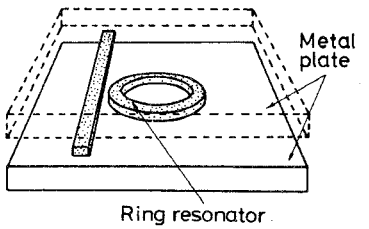

Fig. 9. Structure of Stycast ring resonator.

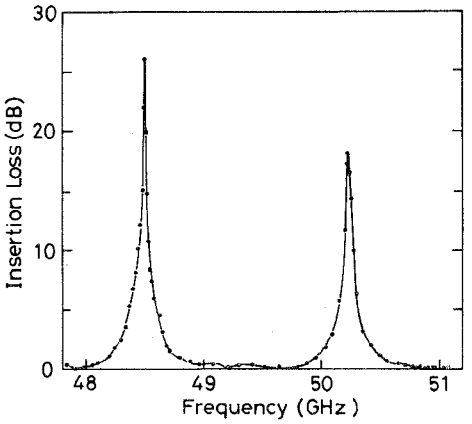

Fig. 10. Measured band-rejection characteristics of Stycast ring resonator with a mean radius of 5 mm and coupling spacing of 0.3 mm.

insulated NRD-guide can probably be attributed to unavoidable experimental errors. It is surprising to see that bending losses are negligible even for a bend of such a small curvature radius as 2 mm, which is about two thirds of the guide wavelength. In the NRD-guide bends of polystyrene dielectric, a considerable amount of reflection occurred for a curvature radius of about one guide wavelength [3]. This clearly shows that high-dielectric material is very suitable for the construction of very sharp bends.

For the two types of open dielectric waveguides, bending losses were around 1 dB. The advantage of the insulated NRD-guide over other dielectric waveguides can be seen by comparing the results of these measurements.

E. Ring Resonator

Ring resonators are important in various filter structures, especially in channel dropping filters [5]. A ring resonator, 5 mm in radius, was fabricated with Stycast (see Fig. 9). A slice of foamed polystyrene was used to support the ring.

The condition for perfect band rejection of the ring resonator is given by [6]

$$e^{-\alpha l} = \sqrt{1 - K^2} \tag{7}$$

where α and l are the attenuation constant and the mean path length of the ring, respectively, and K is the voltage coupling factor between the main guide and the ring. The attenuation constant α consists of the transmission and radiation losses. Since the radiation loss at a bend is negligible in the insulated NRD-guide, α is expected to be small compared to open dielectric waveguides. As to the voltage coupling factor K, the presence of the conducting plates acts to enhance coupling between two dielectric strips [7]. Thus, (7) is satisfied for the insulated NRD-guide provided that the spacing between the ring and the main arm is properly adjusted. In other types of dielectric waveguides, the attenuation constant α is large because of the radiation loss, hence perfect rejection is difficult to achieve.

Measured insertion loss for a ring resonator with a coupling spacing of 0.3 mm is presented in Fig. 10. Maximum insertion loss was about 26 dB at 48.52 GHz and about 19 dB at 50.24 GHz. By changing the coupling spacing between the main arm and the ring, the insertion loss peak could be changed. When the ring touched the main guide, a maximum rejection of about 26 dB was obtained at 50.24 GHz and a rejection of about 15.5 dB was obtained at 48.52 GHz. The measured insertion loss of 26 dB should be compared with a reported value of about 15 dB for an image guide ring resonator [8].

F. Chip Resonator

Since radiation does not occur at any discontinuities in the insulated NRD-guide, small dielectric chips can be expected to operate as high-Q resonators. As a preliminary measurement for the filter fabrication, chip resonators were made of alumina and their resonance characteristics were investigated. A length of alumina strip with 1.5-mm × 1.0-mm transverse dimensions was cut into three parts. The outer two parts served as input and output guides and the inner part, 4.5 mm in length, served as a chip resonator. A slice of foamed polystyrene was used to support each

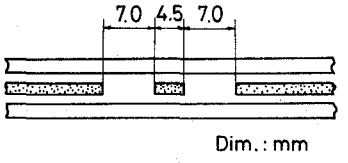

Fig. 11. Side view of alumina chip resonator.

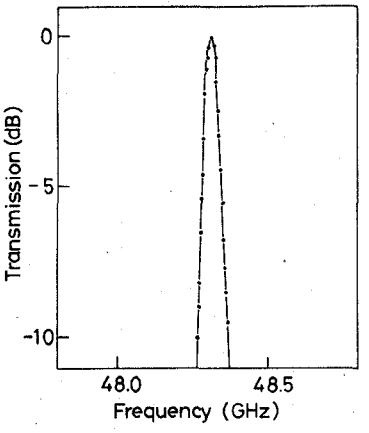

Fig. 12. Measured response of alumina chip resonator.

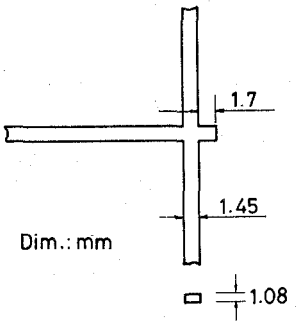

Fig. 13. Structure of Stycast T-junction with a small extension as a matching element.

element in its proper position. Spacing between the chip and each connecting guide was fixed at 7.0 mm. A side view of the structure is shown in Fig. 11 and its measured resonance curve is shown in Fig. 12. The resonance frequency is 48.3 GHz and the Q-factor is about 1070. This value of Q-factor would be adequate to construct insulated NRD-guide filters. When Teflon sheets 0.5 mm in thickness were used as the overlays, the Q-factor was reduced to 710 due to the dielectric loss of Teflon and also due to the increased conduction loss by the requirement that the conducting plate separation be decreased to 2.0 mm in this case. In spite of this reduction of Q-factor, the Teflon overlays are very practical for holding small chips firmly in place.

G. T-Junctions

Although the T-junction is a useful component for millimeter-wave integrated circuits, it is not easy to realize it with conventional dielectric waveguides because a substantial amount of radiation is generated at the junction. With the insulated NRD-guide, however, practical T-junctions can be constructed without much difficulty. Fig. 13 shows

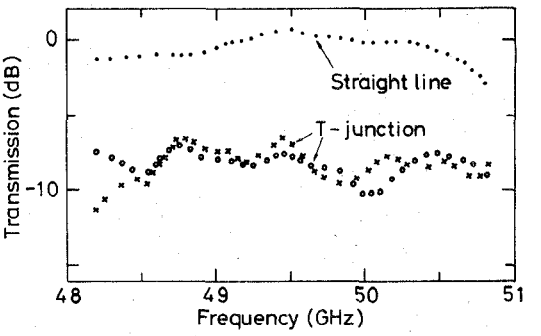

Fig. 14. Output of Stycast T-junction detected at both ends of the main arm, when fed from the stub arm.

a fabricated Stycast T-junction. A small extension of the stub arm serves as a matching element to eliminate the reactive component of the junction impedance. In the present case, the optimum length of the matching element was 1.7 mm. Fig. 14 shows output power levels detected at both ends of the main arm, when fed from the stub arm. The outputs are relatively well balanced, but about 8 dB below that of a straight guide having an equal length. A considerable amount of power was reflected back toward the source. In the course of measurements, the size of the dielectric strip was found to be a critical design parameter for T-junctions of small reflection. Further improvement of the T-junction performance is possible if the size of the strip is carefully optimized.

IV. Conclusions

An improved type of the NRD-guide, called an insulated NRD-guide, is proposed to overcome some difficulties which arise when high-dielectric strips are used in the NRD-guide. Guide wavelengths and transmission losses of the proposed guide were measured at 50 GHz and compared with the theoretical values calculated by the EDC method. The theory suggests that transmission losses of about 2.5 dB/m can be realized with the insulated NRD-guide if high-quality alumina with a loss tangent of approximately 10^{-4} is used. Some basic circuit components such as bends, ring resonators, chip resonators, and T-junctions were also fabricated and tested. They operated as expected without suffering from undesirable radiation at bends and discontinuities. Finally, it is suggested that the concept of the NRD-guide can be generalized to any dielectric object so long as it is symmetrical with respect to the midplane of the waveguide. Dielectric objects of interest include resonators of various shapes, ferrite disks, and even semiconductor elements. Research is being directed toward use of such complicated circuit components.

References

[1] T. Yoneyama and S. Nishida, "Nonradiative dielectric waveguide for millimeter-wave integrated circuits," *IEEE Trans. Microwave Theory Tech.*, vol. MTT-29, pp. 1188–1192, Nov. 1981.

[2] T. Yoneyama and S. Nishida, "Nonradiative dielectric waveguide circuit components," *Int. J. Infrared and Millimeter Waves*, vol. 4, no. 3, 1983.

[3] T. Yoneyama, M. Yamaguchi, and S. Nishida, "Bends in nonradiative dielectric waveguide," *IEEE Trans. Microwave Theory Tech.*, vol. MTT-30, pp. 2146–2150, Dec. 1982.

[4] W. B. Zhou and T. Itoh, "Analysis of trapped image guides using effective dielectric constants and surface impedances," *IEEE Trans. Microwave Theory Tech.*, vol. MTT-30, pp. 2163–2166, Dec. 1983.
[5] T. Itanami and S. Shindo, "Channel dropping filter for millimeter-wave integrated circuits," *IEEE Trans. Microwave Theory Tech.*, vol. MTT-26, pp. 759–764, Oct. 1978.
[6] G. L. Matthaei, L. Yound, and E. M. T. Jones, *Microwave Filters, Impedance-Matching Networks, and Coupling Structures.* New York: MacGraw-Hill, 1964.
[7] T. Yoneyama, N. Tozawa, and S. Nishida, "Coupling characteristics of nonradiative dielectric waveguides," *IEEE Trans. Microwave Theory Tech.*, (submitted).
[8] K. Solbach, "The fabrication of dielectric image lines using casting resins and the properties of the lines in the millimeter-wave range," *IEEE Trans. Microwave Theory Tech.*, vol. MTT-24, pp. 879–881, Nov. 1976.

✤

Tsukasa Yoneyama (S'60–M'64) graduated from Tohoku University, Sendai, Japan, in 1959, and received the M.E. and Ph.D. degrees in electrical communication engineering from the same university in 1961 and 1964, respectively.

He is currently Associate Professor at the Research Institute of Electrical Communication, Tohoku University, where his research interests are concerned with electromagnetic field theory and millimeter-wave integrated circuits.

Dr. Yoneyama is a member of IECE of Japan.

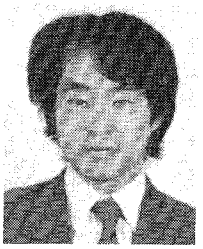

Sadao Fujita was born in Ibaraki prefecture, Japan, on February 27, 1959. He received the B.S. degree from Utsunomiya University, Utsunomiya, Japan, in 1981 and the M.S. degree from Tohoku University, Sendai, Japan, in 1983. He joined the Opto-Electronics Research Laboratory, NEC cooperation in 1983.

Mr. Fujita is a member of IECE of Japan.

✤

Shigeo Nishida (SM'59) was born in Nagoya, Japan, on March 7, 1924. He graduated from Tohoku University, Sendai, Japan, in 1949, and received the Ph.D. degree from the same university in 1959.

He was appointed a Research Associate and an Associate Professor at the Research Institute of Electrical Communication, Tohoku University, in 1949 and 1955, respectively. From 1957 to 1959, on leave of absence from Tohoku University, he joined the Microwave Research Institute of the Polytechnic Institute of Brooklyn, Brooklyn, NY, where he was engaged in research on microwave waveguides and antennas. Since 1964, he has been a Professor at Tohoku University, and his major interests are in microwave and optical wave transmissions.